MiR-637 maintains the balance between adipocytes and osteoblasts by directly targeting Osterix

Jin-fang Zhang[a], Wei-ming Fu[a], Ming-liang He[a,b], Hua Wang[a], Wei-mao Wang[a], Shi-cang Yu[c], Xiu-Wu Bian[c], Jin Zhou[d], Marie C. M. Lin[e,f], Gang Lu[e,f], Wai-sang Poon[e,f], and Hsiang-fu Kung[a,b]

[a]Stanley Ho Centre for Emerging Infectious Diseases, [b]Li Ka Shing Institute of Health Sciences, and [c]Institute of Pathology and Southwest Cancer Center, Southwest Hospital, Third Military Medical University, Chongqing, 400038, P. R. China; [d]First Affiliated Hospital of Harbin Medical University, Hei-Longjiang, 150000, P. R. China; [e]Brain Tumor Center, Neurosurgery, Faculty of Medicine, The Chinese University of Hong Kong, Hong Kong, P. R. China; [f]Prince of Wales Hospital, Shatin, Hong Kong, P. R. China

ABSTRACT **Bone development is dynamically regulated by homeostasis, in which a balance between adipocytes and osteoblasts is maintained. Disruption of this differentiation balance leads to various bone-related metabolic diseases, including osteoporosis. In the present study, a primate-specific microRNA (miR-637) was found to be involved in the differentiation of human mesenchymal stem cells (hMSCs). Our preliminary data indicated that miR-637 suppressed the growth of hMSCs and induced S-phase arrest. Expression of miR-637 was increased during adipocyte differentiation (AD), whereas it was decreased during osteoblast differentiation (OS), which suggests miR-637 could act as a mediator of adipoosteogenic differentiation. Osterix (Osx), a significant transcription factor of osteoblasts, was shown to be a direct target of miR-637, which significantly enhanced AD and suppressed OS in hMSCs through direct suppression of Osx expression. Furthermore, miR-637 also significantly enhanced de novo adipogenesis in nude mice. In conclusion, our data indicated that the expression of miR-637 was indispensable for maintaining the balance of adipocytes and osteoblasts. Disruption of miR-637 expression patterns leads to irreversible damage to the balance of differentiation in bone marrow.**

Monitoring Editor
Marianne Bronner-Fraser
California Institute of Technology

Received: Apr 25, 2011
Revised: Aug 15, 2011
Accepted: Aug 25, 2011

This article was published online ahead of print in MBoC in Press (http://www.molbiolcell.org/cgi/doi/10.1091/mbc.E11-04-0356) on August 31, 2011.

The authors declare no conflict of interest.

Address correspondence to: Hsiang-fu Kung (b110473@mailserv.cuhk.edu.hk) or Gang Lu (lugang@surgery.cuhk.edu.hk).

Abbreviations used: AD, adipocyte differentiation; AKP, alkaline phosphatase; ARS, Alizarin Red staining; BMP2, bone morphogenic protein 2; C/EBPα, CCAAT/enhancer-binding protein α; GAPDH, glyceraldehyde 3-phosphate dehydrogenase; hMSC, human mesenchymal stem cell; hsa, *Homo sapiens*; Lv-Ctrl, lentiviral control; Lv-miR637, lentiviral pre-miR-637 vector; Lv-shmiR-637, lentiviral shRNA of pre-miR637 vector; miRNA, microRNA; MTT, methylthiazolyldiphenyl-tetrazolium bromide; Mu, site-mutated type; NC, negative control; OS, osteoblast differentiation; Osx, Osterix; Osx-si, small specific interfering RNA of Osterix; PBS, phosphate-buffered saline; PPARγ, peroxisome proliferator–activated receptor gamma; qRT-PCR, quantitative real-time PCR; Runx2, runt-related transcription factor 2; shRNA, short-hairpin RNA; SREBP-1c, sterol regulatory element–binding protein 1c; Stat3, signal transducer and activator of transcription 3; WT, wild type.

INTRODUCTION

Osteoporosis is becoming a serious public health problem, as global population aging accelerates. Most patients show an increase in adipocytes in the bone marrow accompanied by bone loss (Meunier *et al*., 1971). Bone marrow fat cells and bone cells share a common progenitor, mesenchymal stem cells, that can differentiate into osteoblasts or adipocytes (Chamberlain *et al*., 2007). Both types of cell maintain homeostasis in the bone marrow and can transdifferentiate under certain conditions (Baksh *et al*., 2004). A balance between the differentiation of adipocytes and osteoblasts in the bone marrow must be maintained for the growth of dynamic connective bone tissue. With increasing age, the balance in differentiation can be disrupted, and an excessive accumulation of bone marrow adipocytes and a decrease in bone volume are observed, resulting in osteoporosis (Tokuzawa *et al*., 2010). Therefore the balance between bone formation and bone marrow adipogenesis might be a therapeutic candidate for the prevention or treatment of osteoporosis, which exhibits deficient bone formation and excessive bone marrow adipogenesis (Nuttall and Gimble, 2000, 2004).

MicroRNAs (miRNAs) are a diverse class of small, noncoding RNA molecules that function as negative gene regulators (Ambros, 2004; Bartel, 2004). Although the physiological functions of most miRNAs are largely unknown, recent evidence has documented a functional contribution of specific miRNAs to stem cell differentiation and development in various tissues and organs (Karp and Ambros, 2005; Tiscornia and Izpisúa Belmonte, 2010). Several miRNAs, such as miR-143, miR-378, miR-27a, miR-26a, miR-29b, miR-125b, miR-133, and miR-135, have been shown to be involved in the differentiation of adipocytes or osteoblasts (Esau *et al.*, 2004; Li *et al.*, 2008, 2009c; Luzi *et al.*, 2008; Mizuno *et al.*, 2008; Kim *et al.*, 2009, 2010; Gerin *et al.*, 2010). Recently, it was shown that overexpression of miR-204 suppressed osteoblast differentiation (OS) and promoted adipocyte differentiation (AD), suggesting that adipoosteoblast differentiation was tightly regulated by some specific miRNAs in human mesenchymal stem cell (hMSCs; Huang *et al.*, 2010).

MiR-637, a primate-specific miRNA, was identified several years ago (Cummins *et al.*, 2006), but no evidence of its functions has been documented to date. In the present study, we investigated the potential involvement of miR-637 in the balance between adipocytes and osteoblasts. We also investigated the potential role of miR-637 on de novo adipogenesis in a murine model. Finally, we explored the underlying functional mechanism of miR-637 in adipoosteogenic differentiation. To the best of our knowledge, this is the first report to demonstrate the role of miR-637 in differentiation.

RESULTS

MiR-637 significantly suppresses cell growth in hMSCs

According to microarray data, miR-638, a primate-specific miRNA in chromosome 19, was highly expressed in human stem cells (Li *et al.*, 2009b). To investigate their functions in hMSCs, we purchased all of the primate-specific miRNAs in chromosome 19, including miR-637, miR-638, miR-639, miR-640, miR-641, miR-642a, and miR-643. The quantitative real-time PCR (qRT-PCR) results showed that the expression of miR-637 and miR-638 in hMSCs was remarkable (Supplemental Figure S1A). We also found that the expression of most miRNAs remained fairly stable during osteoblast differentiation (OS) and adipocyte differentiation (AD); however, miR-637 was significantly down-regulated during OS and up-regulated in AD at day 12 (Figure S1B). We postulated that miR-637 might play a role in the processes of OS and AD.

To study the effect of miR-637 on the differentiation of hMSCs, we first examined its effect on cell growth. MiR-637, anti-miR-637, and a negative control (NC) were transiently transfected into hMSCs, and cell growth was assayed. As shown in Figure 1A, miR-637 inhibited cell growth in hMSCs by 23% ($p < 0.01$), whereas anti-miR-637 promoted cell growth by 17% ($p < 0.01$). In contrast, the NC had no effect, indicating the effect of miR-637 was strongly specific.

Following the investigation of miR-637–mediated growth inhibition, we transfected hMSCs with miR-637 and anti-miR-637 and examined cell cycle distribution. Compared with NC, hMSC cells transfected with miR-637 displayed an increased percentage of cells in the S phase and fewer cells in the G1 phase (Figure 1B; $p < 0.01$). In addition, no significant difference in cell cycle distribution was observed in NC and anti-miR-637–transfected cells. These results suggested that the growth-suppressive effect of miR-637 was partly due to S-phase arrest.

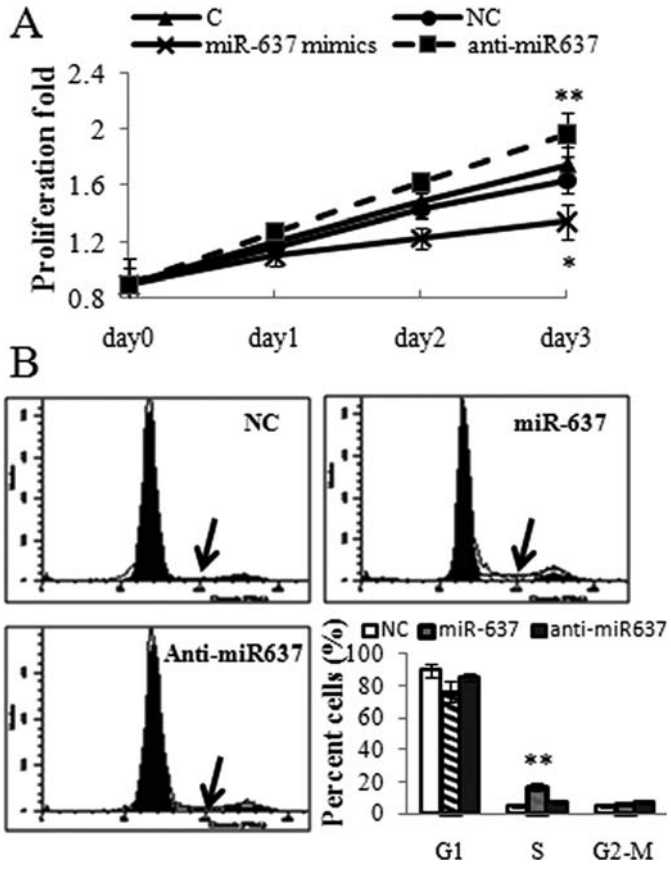

FIGURE 1: MiR-637 inhibited proliferation of hMSCs and induced cell arrest. (A) The effect of miR-637 on cell growth was measured by MTT assay on 3 serial days. (B) The representative images for cell cycle distribution of hMSCs transfected with miRNAs for 72 h. *, $p < 0.05$ vs. NC; **, $p < 0.01$ vs. NC.

Spatial-temporal expression pattern of miR-637 during AD and OS

To identify the effect of miR-637 on differentiation, we assayed the endogenous miR-637 expression pattern during AD and OS. As shown in Figure 2, A and B, miR-637 expression increased during AD and decreased during OS. The expression of DAPK3, the host gene of miR-637, increased during AD and decreased during OS (Figure 2, C and D).

In addition, we examined miR-637 expression in human bone marrow MSCs from two groups of individuals. The results showed that miR-637 expression levels were much higher in hMSCs derived from older subjects (>60 yr of age) who had slight or severe osteoporosis, than in those from younger subjects (<30 yr of age; Figure 2E).

Enforced miR-637 promoted AD and suppressed OS

Next, we used lentiviral vectors to stably restore and silence the expression of miR-637 in hMSCs (Figure S2). AD was induced in these infected cells and adipocytes were stronger in lentiviral pre-miR-637 vector (Lv-miR-637)–infected and weaker in lentiviral short-hairpin (shRNA) of pre-miR637 vector (Lv-shmiR637)–infected cells (Figure 3A). Quantitative analysis of adipocytes showed that miR-637 promoted adipocytes by 118% ($p < 0.01$), while shmiR-637 suppressed adipocytes by 27% in comparison with the lentiviral control (Lv-Ctrl; Figure 3B). Peroxisome proliferator–activated receptor gamma (PPARγ), the main regulator of adipogenesis, was significantly increased in Lv-miR-637–infected hMSCs, and simultaneously

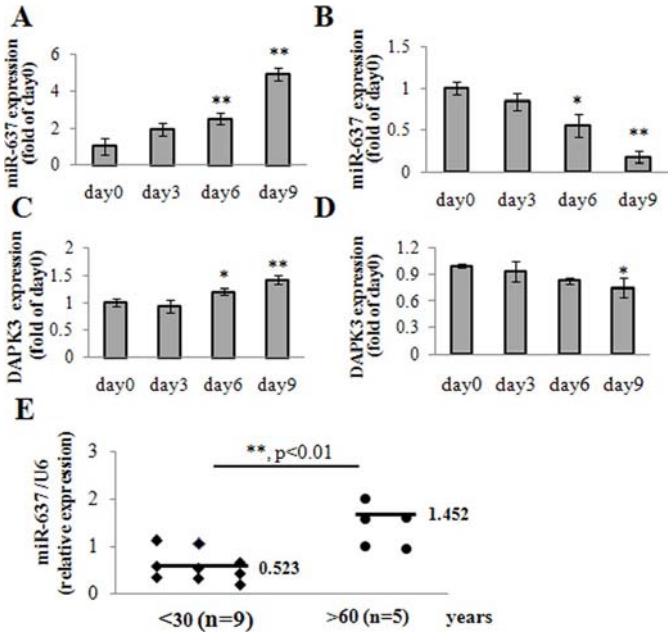

FIGURE 2: Spatial-temporal expression pattern of miR-637. (A) The endogenous expression of miR-637 was increased during AD in hMSCs. (B) MiR-637 expression was decreased during OS. The host gene, DAPK3, was up-regulated during AD (C) and down-regulated during OS (D). (E) MiR-637 expression was higher in bone marrow hMSCs from the older than the younger group ($p < 0.01$). *, $p < 0.05$ vs. day 0; **, $p < 0.01$ vs. day 0.

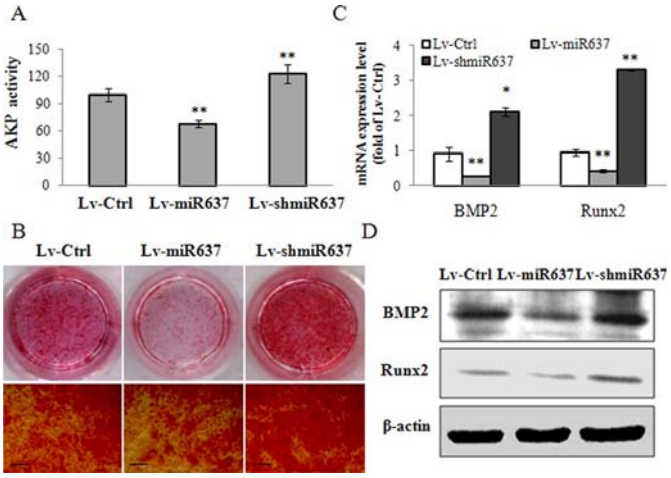

FIGURE 4: The enforced expression of miR-637 suppressed osteoblasts in hMSCs. (A) AKP activity was measured in Lv-Ctrl– and Lv-miR-637–infected hMSCs. (B) Calcium nodules were displayed using ARS staining. (C and D) MiR-637 suppressed the expressions of BMP2 and Runx2 in mRNA (C) and proteins (D). *, $p < 0.05$ vs. Lv-Ctrl; **, $p < 0.01$ vs. Lv-Ctrl.

inhibited in Lv-shmiR-637–infected cells in mRNA and proteins (Figure 3C). Furthermore, other adipogenic markers, including CCAAT/enhancer–binding protein α (C/EBPα) and sterol regulatory element–binding protein 1c (SREBP-1c), were also enhanced by Lv-miR-637, but were down-regulated by Lv-shmiR-637 (Figure 3D).

On the other hand, we also investigated the effect of miR-637 on osteogenesis of hMSCs. The alkaline phosphatase (AKP) activity, an early marker of osteoblasts, was shown to be decreased by 32% in Lv-miR-637–infected cells but increased by 22% in Lv-shmiR-637–infected cells (Figure 4A). The evaluation of calcium nodules demonstrated that Lv-miR-637 suppressed, while Lv-shmiR-637 enhanced, osteoblasts (Figure 4B). Moreover, the expression of bone morphogenic protein 2 (BMP2) and runt-related transcription factor 2 (Runx2) was down-regulated by Lv-miR637 but promoted by Lv-shmiR-637in mRNA (Figure 4C) and proteins (Figure 4D).

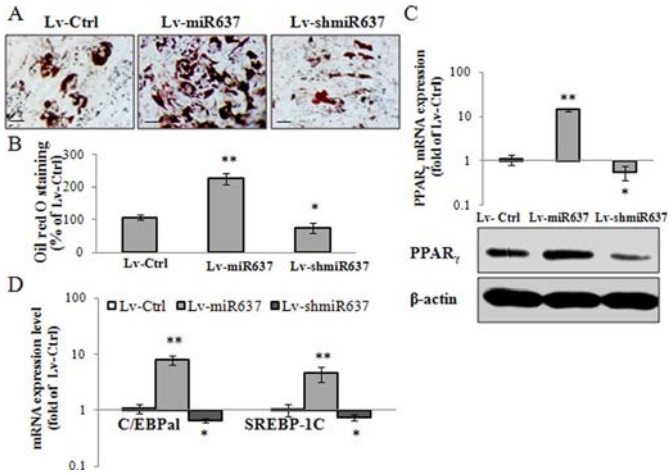

FIGURE 3: The enforced expression of miR-637 promoted adipogenesis in hMSCs. (A) Adipocytes were evaluated by oil red O staining in Lv-Ctrl– and Lv-miR-637–infected hMSCs. Scale bar: 50 μm. (B) Quantitative analyses were performed by measurement of OD at 510 nm. (C) MiR-637 promoted PPARγ expression at mRNA and protein levels. (D) Other adipogenic markers, such as C/EBPα and SREBP-1c, were promoted by miR-637. *, $p < 0.05$ vs. Lv-Ctrl; **, $p < 0.01$ vs. Lv-Ctrl.

Osterix was a direct target of miR-637 in hMSCs

As is well known, miRNAs exert function through suppressing the expression of their target gene(s). To explore the mechanism underlying the adipoosteogenic differentiation balance maintained by miR-637, we performed a bioinformatics analysis using Targetscan (www.targetscan.org; Grimson *et al.*, 2007), miRanda (www.microrna.org; Betel *et al.*, 2010), and Findtar (http://bio.sz.tsinghua.edu.cn; Ye *et al.*, 2008) for the putative mRNA targets. Although hundreds of different targets were predicted by each program, the common targets associated with adipocyte and osteoblast predicted by the three programs were Osterix (Osx) and the signal transducer and activator of transcription 3 (Stat3). In our biological experiments, the latter was demonstrated by luciferase reporter assays to be a pseudotarget of miR-637 (unpublished data). The three programs all predicted that the binding sequence in 3′UTR of Osx was a very good match for the miR-637 seed. To verify this prediction, the target sequence (nt 387–713) of Osx 3′UTR (Wt) or the site-mutated sequence (Mu; the base that is underlined in Figure 5A) was cloned into the luciferase reporter vector pMIR (Figure 5A). Cos-7 cells were then cotransfected with WT vector and miRNA mimics, and the results showed a significant decrease in luciferase activity in miR-637–transfected cells compared with NC (Figure 5B; $p < 0.01$). The activity of the Mu vector was unaffected by a simultaneous transfection with miR-637 (Figure 5B). Moreover, cotransfection with anti-miR-637 and the WT or Mu vector had no significant effect on luciferase activity (Figure 5B). Furthermore, as shown in Figure 5, C and D, ectopic expression of miR-637 led to a decrease in Osx in mRNA and proteins. Moreover, suppression of endogenous miR-637 resulted in the up-regulation of Osx in hMSCs.

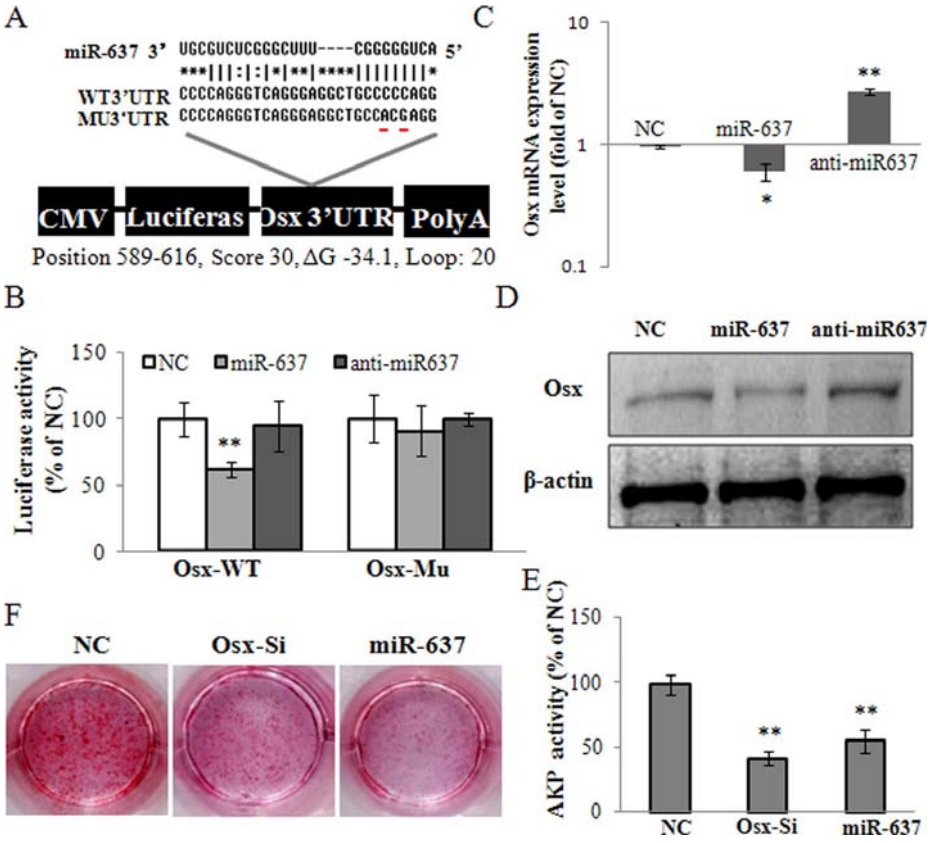

FIGURE 5: Osx was a direct target of miR-637. (A) Schematic diagram of the predicted miR-637 binding sites of the Osx 3′UTR-containing reporter constructs; the underlined base is the site-mutated sequence. (B) Luciferase reporter assays in Cos-7 cells. Luciferase reporter constructs containing a wild-type and site-mutated Osx 3′UTR were transfected into Cos-7 cells. The relative suppression of the firefly luciferase expression was standardized to total protein. (C) The mRNA expression levels of Osx were depressed by miR-637 and improved by anti-miR-637. (D) The protein expression levels of Osx were decreased in miR-637–transfected hMSC cells and enhanced in anti-miR-637–transfected cells using Western blotting. (E) AKP activity was suppressed by Osx-si. (F) Calcium nodules were decreased by Osx-si. *, $p < 0.05$ vs. NC; **, $p < 0.01$ vs. NC.

To further confirm the positive effect of Osx on osteogenic differentiation, small specific interfering RNA of Osx (Osx-si) was transfected into hMSCs and osteogenesis was assayed. As shown in Figure 5E, AKP activity was inhibited and calcium nodules were strongly suppressed by Osx-si (Figure 5F).

MiR-637 maintained the balance between adipocyte and osteoblast differentiation

In the following experiments discussed, we imitated the adipoosteogenic differentiation of hMSCs using a semi-AD and semi-OS induction system as reported previously (Liu *et al.*, 2009). As shown in Figure 6A, fewer red calcium nodules and more adipocyte drops (red drops) were observed in Lv-miR-637–infected hMSCs, which contrasted with the converse results observed in Lv-shmiR-637–infected cells. In addition, the expressions of BMP2 and Runx2 were decreased and PPARγ was increased in Lv-miR-637–infected cells, whereas Lv-shmiR-637 enhanced the expression of BMP2 and Runx2 and suppressed that of PPARγ in the semiinduction system (Figure 6B).

MiR-637 promoted de novo adipocytes in athymic mice

To explore whether miR-637 had an effect on adipogenesis in vivo, a de novo adipogenic mouse model was used. Lv-Ctrl– or Lv-miR637–infected hMSCs were injected subcutaneously into mice twice a week for the first 2 wk. A remarkable increase in adipose tissue was observed in nude mice following injection with Lv-miR-637–infected hMSCs, whereas little adipose tissue was formed de novo with Lv-Ctrl–infected hMSCs (Figure 7A). Hemotoxylin-eosin staining revealed a striking enhancement of the quantity and size of adipocytes induced by Lv-miR-637 (Figure 7B). Weights of fat pads were measured, and the results showed that fat formation was increased by miR-637 overexpression (Figure 7C). Furthermore, Lv-miR-637 promoted the mRNA expression levels of PPARγ, C/EBPα, and SREBP-1c in de novo adipose tissue (Figure 7D). It must be emphasized that these primers of PPARγ, C/EBPα, and SREBP-1c were human-specific. Thus miR-637 overexpression facilitated de novo adipogenesis in nude mice.

DISCUSSION

Osteoporosis and the increased risk of fragile fractures are one of the characteristic manifestations of aging (Rodríguez *et al.*, 1999). Not only a decrease in osteoblasts, but also an increase in adipocytes in the bone marrow, may contribute to this bone-associated metabolic disease (Meunier *et al.*, 1971; Koo *et al.*, 1998). Recent studies have shown that bone marrow adipocytes not only suppress osteoblasts, but might also promote bone resorption by the secretion of inflammatory cytokines and the recruitment of osteoclasts (Weisberg *et al.*, 2003). Therefore, in addition to stimulating bone formation, the suppression of adipogenesis may be of considerable significance for the prevention and treatment of osteoporosis.

MiR-637 is a primate-specific miRNA that has been found in four primate species (Lin *et al.*, 2010). Our results confirmed that miR-637 was absent in rat and mouse MSCs (unpublished data). Although miR-637 was discovered several years ago, its functions, especially in cell death and differentiation, remain unknown. Our study first demonstrated that miR-637 could moderately inhibit cell growth and induce S-phase arrest in hMSC cells (Figure 1). In addition, we also found that the expression of miR-637 was increased during AD, whereas it was decreased during OS (Figure 2). To determine the precise role of miR-637 in differentiation, we tested the effect of miR-637 on adipocytes and osteoblasts. Our results showed that miR-637 promoted the formation of adipocytes and conversely inhibited that of osteoblasts (Figures 3 and 4), suggesting that it maintained the differentiation balance between AD and OS. As a primate-specific miRNA, the function of miR-637 was regarded to be poorly conserved in rodents. Some homologous miRNAs in mice that act similarly to hsa (*Homo sapiens*)-miR-637 in hMSCs may exist, but we have not found such a miRNA in the miRbase (www.mirbase.org) to date.

Because adipogenesis and osteogenesis are very complicated systems in the bone marrow, to demonstrate further the function of miR-637 in maintaining the differentiation balance, we used a semi-induction system to mimic the homeostasis in bone marrow as

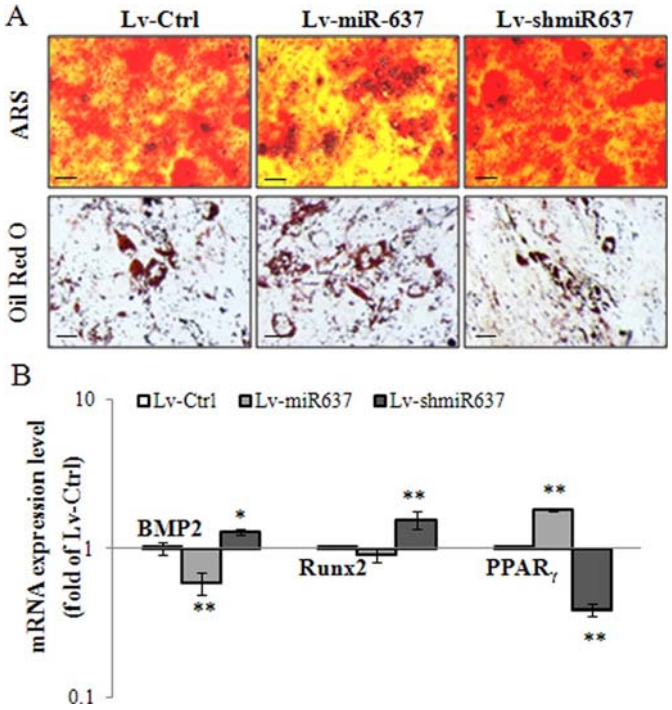

FIGURE 6: MiR-637 maintained the balance between adipoosteogenic differentiation. (A) MiR-637 enhanced adipocytes and suppressed osteoblasts as visualized using ARS and oil red O staining, respectively. (B) The critical regulators, such as PPARγ, BMP2, and Runx2, were assayed by qRT-PCR. *, $p < 0.05$ vs. Lv-Ctrl; **, $p < 0.01$ vs. Lv-Ctrl.

described previously (Liu *et al.*, 2009). The enforced overexpression of miR-637 enhanced adipocytes while it decreased osteoblasts. Concomitantly, shmiR-637 stimulated osteogenesis and reduced adipogenesis (Figure 5). These findings suggested that miR-637 could be a therapeutic candidate for osteoporosis due to its capacity to maintain the balance between AD and OS.

In this paper, we describe a novel method for the knockdown of miR-637: the lentiviral vector with shRNA of pre-miR-637. In a previous report, we constructed the lentiviral vector with miRNA-expression cassettes to overexpress miR-122a (Diao *et al.*, 2010). In this study, we designed shRNA of miR-637 based on the stem loop of pre-miR-637. The constructed lentiviral pre-miR-637 and shmiR-637 vectors easily infected more than 90% of hMSCs (Figure S2A), and the internal expression of mature miR-637 was strongly enforced or silenced (Figure S2B). Therefore successful construction of these vectors provided us with an efficient and inexpensive way to introduce miRNAs into cultured cells, which may facilitate gain-of-function and loss-of-function studies with any interest in miRNAs.

Osx, a novel zinc finger–containing transcription factor, was identified as a critical regulator of bone formation and OS (Nakashima *et al.*, 2002). In humans, the Osx (Sp7) gene, like its murine orthologue, showed osteoblast-specific expression in vivo (Gao *et al.*, 2004). Osx transcription was stimulated by BMP2 and has been shown to be involved in BMP2-induced OS in hMSCs (Lee *et al.*, 2003; Celil *et al.*, 2005; Ryoo *et al.*, 2006). In our studies, bioinformatics analysis predicted that Osx was a direct target of miR-637and biological evidence demonstrated this in hMSCs (Figure 5). Osx is specifically expressed in all osteoblasts. As a downstream gene of Runx2, Osx is required for the differentiation of preosteoblasts into mature osteoblasts (Nishio *et al.*, 2006). In Osx-null embryos, cartilage is formed normally, but the embryos totally lack bone formation (Zhang *et al.*, 2008). Our data confirmed that Osx knockdown suppressed osteoblasts in hMSCs, which was similar to the phenotypes induced by miR-637 restoration. These results suggested that miR-637–induced differentiation was at least partly mediated by direct suppression of Osx expression.

We discerned the molecular mechanism involved in the adipoosteogenic differentiation induced by miR-637 in an in vitro study. Furthermore, ectopic de novo adipocyte differentiation was applied to evaluate the effect of miR-637 on adipocytes in vivo. Our data revealed that Lv-miR637–infected hMSCs formed a remarkable amount of fat tissue and large adipocyte drops. Simultaneously, these cells had higher expression levels of PPARγ, C/EBPα, and SREBP-1c (Figure 7). Therefore miR-637 achieved beneficial adipocyte differentiation in hMSCs by suppressing Osx expression. This, therefore, suggested that miR-637 probably acted as a mediator to maintain the balance between AD and OS.

In conclusion, we demonstrated that miR-637 promoted adipocytes and suppressed osteoblasts, indicating that miR-637 maintains the constitutive balance between adipogenesis and osteogenesis in hMSCs derived from bone marrow. When that balance is disrupted, adipocytes are stimulated and osteoblasts are suppressed. Therefore primate-specific miR-637 may be a promising therapeutic agent for osteoporosis or obesity.

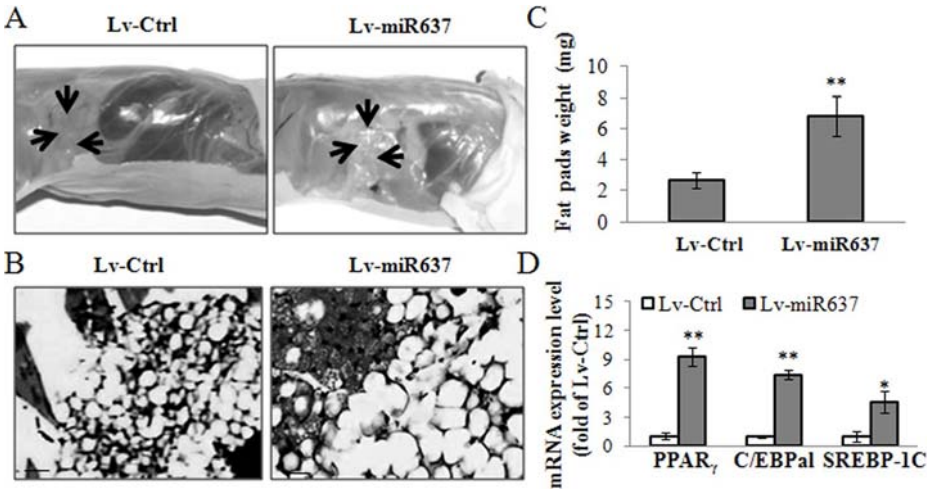

FIGURE 7: MiR-637 promoted de novo adipose tissue formation in nude mice. (A) Nude mice were injected with Lv-Ctrl– or Lv-miR637–infected hMSCs. Fat pad sections were retrieved 6 wk later. (B) Hemotoxylin-eosin staining of representative sections are shown. Scale bar: 50 μm. (C) Quantitative analyses of fat pad weight. (D) Some regulators were analyzed. *, $p < 0.05$, vs. Lv-Ctrl; **, $p < 0.01$ vs. Lv-Ctrl.

MATERIALS AND METHODS

Cell culture and induction of OS and AD

Nine bone marrow samples from young subjects (<30 yr) and five bone marrow samples from older subjects (>60 yr) with slight or severe osteoporosis were obtained, from which hMSCs were isolated and identified by cell surface markers (Zhang *et al.*, 2009). Briefly, bone marrow was aspirated and hMSCs were cultured in minimum essential

medium, alpha, supplemented with 10% fetal bovine serum, 2 mM L-glutamine, 100 U/ml penicillin, and 100 µg/ml streptomycin, and were incubated in a humidified atmosphere of 5% CO_2 at 37°C.

OS and AD were induced according to a published protocol (Li *et al.*, 2009a; Zhang *et al.*, 2010). OS medium was supplemented with 10^{-8} M dexamethasone, 50 µg/ml ascorbic acid 2-phosphate, and 10 mM glycerol 2-phosphate (Sigma-Aldrich, St. Louis, MO). AD medium was supplemented with 10^{-7} M dexamethasone, 10 µg/ml insulin, and 0.45 mM 3-isobutyl-1-methyl-xanthine (Sigma). hMSCs were seeded onto a 12-well plate at a density of 5×10^5 cells per well, and the culture medium was changed to OS or AD medium after 24 h. The cells were then incubated at 37°C with 5% CO_2, and the medium was changed every 3 d.

miRNA transfection

miRNAs were transfected at a concentration of 100 nM using Lipofectamine 2000 (Invitrogen, Carlsbad, CA). The miR-637 mimic, a nonspecific negative control, anti-miR-637, and Osx-si were all purchased from GenePharma (Shanghai, China).

The sequence of Osx-si was 5′UUGCCCCAAGAUGUCUAUAAACCCAAG3′.

Construction of lentiviral plasmid, lentivirus production and infection

A 295 base pair fragment of pre-miR-637 encompassing the stem loop was amplified and then cloned into the lentiviral vector pLVTHM. Another lentiviral vector for shRNA delivery of the pre-miR-637 stem loop was obtained as described previously (Zhang *et al.*, 2011a). The production and purification of the lentivirus were also performed as described previously (Diao *et al.*, 2010). A lentiviral vector that expressed a scrambled RNA was used as a control. The packaged lentiviruses were named Lv-miR-637 and Lv-shmiR-637, respectively.

Cell growth and cell cycle analysis

Cells were plated in 96-well plates at 3×10^3 per well and were transfected with miRNAs. After transfection, the cells were cultured for 24, 48, and 72 h. The effect of miR-637 on cell growth and viability was determined by the methylthiazolyldiphenyl-tetrazolium bromide (MTT) assay as described previously (Tsang and Kwok, 2009). For cell cycle analysis, cells were plated in 6-well plates at 2×10^5 per well and transfected with miRNAs. At 48 h after transfection, the cell cycle distribution was analyzed using propidium iodide staining and flow cytometry as described previously (Singh *et al.*, 2004).

RNA extraction, reverse transcription, and qRT-PCR

The total RNA was extracted by using Trizol reagent (Invitrogen). For the miR-637 expression assay, total RNA was reversely transcribed using the NCode miRNA First-Strand cDNA Synthesis kit (Invitrogen). To measure the mRNA levels of Osx and other genes, total RNA was reversely transcribed using the ImProm-II Reverse Transcription System (Promega, Madison, WI). All the qRT-PCR samples were performed using SYBR Green PCR Master Mix (Roche, Indianapolis, IN) on an Applied Biosystems 7500 Real-Time PCR System (Bedford, MA). The primers used are listed in Supplemental Table SI. U6 or glyceraldehyde 3-phosphate dehydrogenase (GAPDH) was used as an endogenous control, and fold changes were calculated by means of relative quantification ($2^{-\Delta\Delta Ct}$; Lu *et al.*, 2011).

AKP analysis

hMSCs were seeded at a density of 2×10^5 cells per well onto a 24-well plate, and OS was induced within 24 h. Cell lysates were collected, and AKP activity was assayed as reported previously (Zhang *et al.*, 2009).

Adipocyte assay: oil red O staining

The hMSCs were gently washed twice with phosphate-buffered saline (PBS), and then fixed in 4% paraformaldehyde (micrograms/volume [ml] [m/V]) for 10 min. The samples were then washed twice with deionized water, and 1/3 saturated oil red O staining was carried out for 1 h and the samples were again washed twice. Isopropanol was finally added to dissolve the oil red O, and the optical density (OD) value was measured under 510 nm.

Mineralization assay: Alizarin Red staining

After hMSCs were fixed in 4% paraformaldehyde (m/V) for 10 min, samples were evaluated by ARS staining. Briefly, cells were stained with 2% Alizarin Red staining (ARS, pH 4.1) for 15 min and then washed twice. The orange and red positions were recognized as calcium nodules.

Western blotting

Cell lysates were separated by SDS–PAGE (10%) and transferred to polyvinylidene fluoride membranes (Millipore, Billerica, MA). The membranes were blocked with 5% skim milk for 1 h and incubated with mouse monoclonal anti-BMP2, anti- Runx2 (Abcam, Cambridge, MA), rabbit polyclonal anti-PPARγ (Santa Cruz Biotechnology, Santa Cruz, CA), and anti-Osx (Santa Cruz) antibodies. This was then followed by incubation with the corresponding horseradish peroxide-labeled IgG (1:5000) for 1 h. Finally, chemiluminescence (ECL; PerkinElmer) was used to visualize the results, and GAPDH was used as an internal control.

Luciferase assays

Luciferase assays were performed according to a previously published protocol (He *et al.*, 2010; Zhang *et al.*, 2011b). In brief, the 3′ untranslated region (UTR) of Osx (nt 387–713), and its corresponding mutated 3′UTR were amplified by PCR using the primers shown in Table SI. The target sequences were cloned into the pMIR reporter vector (Promega). Cos-7 cells were seeded onto a 24-well plate at a density of 1×10^5, and cotransfection was performed. The firefly luciferase activities were measured using the Luciferase Reporter Assay System (Promega), and each experiment was repeated in triplicate. The luciferase activity was normalized by total protein content.

De novo adipose formation model

The treatment and usage of young athymic nude mice (females, 4–6 wk, from the Chinese University of Hong Kong) complied with the guidelines of the Animal Experimental Ethics Committee of the Chinese University of Hong Kong. Each experimental group consisted of five animals. hMSCs were infected with Lv-miR-637 or the lentivirus control (Lv-Ctrl) to induce adipogenesis for 3 d, and were then collected and injected subcutaneously into the nude mice (1×10^8 cells/mouse). Six weeks later, five mice from each group were killed, and transplants were retrieved, fixed in 10% formalin overnight, and embedded in paraffin. Sections (5 µm) of embedded samples were stained with hemotoxylin-eosin.

Statistical analysis

Data are expressed as mean ± SD. Statistical analysis was performed using the independent *t* test. A p value of <0.05 was considered to be statistically significant.

ACKNOWLEDGMENTS

This work was supported by the Li Ka Shing Institute of Health Sciences and the conjoined innovation fund of Chinese University of Hong Kong and Science & Technology Office of Hei-Longjiang Province (PG09J003).

REFERENCES

Ambros V (2004). The functions of animal microRNAs. Nature 431, 350–355.

Baksh D, Song L, Tuan RS (2004). Adult mesenchymal stem cells: characterization, differentiation, and application in cell and gene therapy. J Cell Mol Med 8, 301–316.

Bartel DP (2004). MicroRNAs: genomics, biogenesis, mechanism, and function. Cell 116, 281–297.

Betel D, Koppal A, Agius P, Sander C, Leslie C (2010). Comprehensive modeling of microRNA targets predicts functional non-conserved and non-canonical sites. Genome Biol 11, R90.

Celil AB, Hollinger JO, Campbell PG (2005). Osx transcriptional regulation is mediated by additional pathways to BMP2/Smad signaling. J Cell Biochem 95, 518–528.

Chamberlain G, Fox J, Ashton B, Middleton J (2007). Concise review: mesenchymal stem cells: their phenotype, differentiation capacity, immunological features, and potential for homing. Stem Cells 25, 2739–2749.

Cummins JM *et al.* (2006). The colorectal microRNAome. Proc Natl Acad Sci USA 103, 3687–3692.

Diao S, Zhang JF, Wang H, He ML, Lin MC, Chen Y, Kung HF (2010). Proteomic identification of microRNA-122a target proteins in hepatocellular carcinoma. Proteomics 10, 3723–3731.

Esau C *et al.* (2004). MicroRNA-143 regulates adipocyte differentiation. J Biol Chem 279, 52361–52365.

Gao Y, Jheon A, Nourkeyhani H, Kobayashi H, Ganss B (2004). Molecular cloning, structure, expression, and chromosomal localization of the human Osterix (SP7) gene. Gene 341, 101–110.

Gerin I, Bommer GT, McCoin CS, Sousa KM, Krishnan V, MacDougald OA (2010). Roles for miRNA-378/378* in adipocyte gene expression and lipogenesis. Am J Physiol Endocrinol Metab 299, E198–E206.

Grimson A, Farh KK, Johnston WK, Garrett-Engele P, Lim LP, Bartel DP (2007). MicroRNA targeting specificity in mammals: determinants beyond seed pairing. Mol Cell 27, 91–105.

He J *et al.* (2010). MiRNA-mediated functional changes through co-regulating function related genes. PLoS One 5, e13558.

Huang J, Zhao L, Xing LP, Chen D (2010). MicroRA-204 regulates Runx2 protein expression and mesenchymal progenitor cell differentiation. Stem Cells 28, 357–364.

Karp X, Ambros V (2005). Developmental biology. Encouraging miRNAs in cell fate signaling. Science 310, 1288–1289.

Kim SY, Kim AY, Lee HW, Son YH, Lee GY, Lee JW, Lee YS, Kim JB (2010). MiR-27a is a negative regulator of adipocyte differentiation via suppressing PPARgamma expression. Biochem Biophys Res Commun 392, 323–328.

Kim YJ, Bae SW, Yu SS, Bae YC, Jung JS (2009). MiR-196a regulates proliferation and osteogenic differentiation in mesenchymal stem cells derived from human adipose tissue. J Bone Miner Res 24, 816–825.

Koo KH, Dussault R, Kaplan P, Kim R, Ahn IO, Christopher J, Song HR, Wang GJ (1998). Age-related marrow conversion in the proximal metaphysis of the femur: evaluation with T1-weighted MR imaging. Radiology 206, 745–748.

Lee MH, Kwon TG, Park HS, Wozney JM, Ryoo HM (2003). BMP-2-induced Osterix expression is mediated by Dlx5 but is independent of Runx2. Biochem Biophys Res Commun 309, 689–694.

Li G *et al.* (2009a). Comparative proteomic analysis of mesenchymal stem cells derived from human bone marrow, umbilical cord, and placenta: implication in the migration. Proteomics 9, 20–30.

Li SS, Yu SL, Kao LP, Tsai ZY, Singh S, Chen BZ, Ho BC, Liu YH, Yang PC (2009b). Target identification of miRNAs expressed highly in human embryonic stem cells. J Cell Biochem 106, 1020–1030.

Li Z, Hassan MQ, Volinia S, van Wijnen AJ, Stein JL, Croce CM, Lian JB, Stein GS (2008). A microRNA signature for a BMP2-induced osteoblast lineage commitment program. Proc Natl Acad Sci USA 105, 13906–13911.

Li Z, Hassan MQ, Jafferji M, Garzon R, Garzon R, Croce CM, van Wijnen AJ, Stein GS, Lian JB (2009c). Biological functions of miR-29b contribute to positive regulation of osteoblast differentiation. J Biol Chem 284, 15676–15684.

Lin S, Cheung WK, Chen S, Lu G, Wang Z, Xie D, Li K, Lin MC, Kung HF (2010). Computational identification and characterization of primate-specific microRNAs in human genome. Comput Biol Chem 34, 232–241.

Liu GZ, Vijayakumar S, Grumolato L, Arroyave R, Qiao HF, Akiri G, Aaronson SA (2009). Canonical Wnts function as potent regulators of osteogenesis by human mesenchymal stem cell. J Cell Biol 185, 67–75.

Lu J *et al.* (2011). MiR-26a inhibits cell growth and tumorigenesis of nasopharyngeal carcinoma through repression of EZH2. Cancer Res 71, 225–233.

Luzi E, Marini F, Sala SC, Tognarini I, Galli G, Brandi ML (2008). Osteogenic differentiation of human adipose tissue-derived stem cells is modulated by the miR-26a targeting of the SMAD1 transcription factor. J Bone Miner Res 23, 287–289.

Meunier P, Aaron J, Edouard C, Vignon G (1971). Osteoporosis and the replacement of cell populations of the marrow by adipose tissue. A quantitative study of 84 iliac bone biopsies. Clin Orthop Relat Res 80, 147–154.

Mizuno Y *et al.* (2008). MiR-125b inhibits osteoblastic differentiation by down-regulation of cell proliferation. Biochem Biophys Res Commun 368, 267–272.

Nakashima K, Zhou X, Kunkel G, Zhang Z, Deng JM, Behringer RR, de Crombrugghe B (2002). The novel zinc finger-containing transcription factor osterix is required for osteoblast differentiation and bone formation. Cell 108, 17–29.

Nishio Y, Dong Y, Paris M, O'Keefe RJ, Schwarz EM, Drissi H (2006). Runx2-mediated regulation of the zinc finger Osterix/Sp7 gene. Gene 372, 62–70.

Nuttall ME, Gimble JM (2000). Is there a therapeutic opportunity to either prevent or treat osteopenic disorders by inhibiting marrow adipogenesis?. Bone 27, 177–184.

Nuttall ME, Gimble JM (2004). Controlling the balance between osteoblastogenesis and adipogenesis and the consequent therapeutic implications. Curr Opin Pharmacol 4, 290–294.

Rodríguez JP, Garat S, Gajardo H, Pino AM, Seitz G (1999). Abnormal osteogenesis in osteoporotic patients is reflected by altered mesenchymal stem cells dynamics. J Cell Biochem 75, 414–423.

Ryoo HM, Lee MH, Kim YJ (2006). Critical molecular switches involved in BMP-2-induced osteogenic differentiation of mesenchymal cells. Gene 366, 51–57.

Singh SV, Herman-Antosiewicz A, Singh AV, Lew KL, Srivastava SK, Kamath R, Brown KD, Zhang L, Baskaran R (2004). Sulforaphane-induced G2/M phase cell cycle arrest involves checkpoint kinase 2-mediated phosphorylation of cell division cycle 25C. J Biol Chem 279, 25813–25822.

Tiscornia G, Izpisúa Belmonte JC (2010). MicroRNAs in embryonic stem cell function and fate. Genes Dev 24, 2732–2741.

Tokuzawa Y *et al.* (2010). Id4, a new candidate gene for senile osteoporosis, acts as a molecular switch promoting osteoblast differentiation. PLoS Genet 6, e1001019.

Tsang WP, Kwok TT (2009). The miR-18a* microRNA functions as a potential tumor suppressor by targeting on K-Ras. Carcinogenesis 30, 953–959.

Weisberg SP, McCann D, Desai M, Rosenbaum M, Leibel RL, Ferrante AW Jr (2003). Obesity is associated with macrophage accumulation in adipose tissue. Clin Invest 112, 1796–808.

Ye W, Lv Q, Wong CK, Hu S, Fu C, Hua Z, Cai G, Li G, Yang BB, Zhang Y (2008). The effect of central loops in miRNA: MRE duplexes on the efficiency of miRNA-mediated gene regulation. PLoS One 3, e1719.

Zhang C, Cho K, Huang Y, Lyons JP, Zhou X, Sinha K, McCrea PD, de Crombrugghe B (2008). Inhibition of Wnt signaling by the osteoblast-specific transcription factor Osterix. Proc Natl Acad Sci USA 105, 6936–6941.

Zhang JF, Li G, Meng CL, Dong Q, Chan CY, He ML, Leung PC, Zhang YO, Kung HF (2009). Total flavonoids of *Herba Epimedii* improves osteogenesis and inhibits osteoclastogenesis of human mesenchymal stem cells. Phytomedicine 16, 521–529.

Zhang JF, Li G, Chan CC, Meng CL, Lin MC, Chen YC, He ML, Leung PC, Kung HF (2010). Flavonoids of *Herba Epimedii* regulate osteogenesis of human mesenchymal stem cells through BMP and Wnt/β-catenin signaling pathway. Mol Cell Endocrinol 314, 70–74.

Zhang JF *et al.* (2011a). Primate-specific miRNA-637 blocks Stat3 phosphorylation by targeting autocrine leukemia inhibitory factor in hepatocellular carcinoma. Hepatology (*in press*); doi: 10.1002/hep.24595.

Zhang JF *et al.* (2011b). MiRNA-20a promotes osteogenic differentiation of human mesenchymal stem cells by co-regulating BMP signaling. RNA Biol 8, 1–10.